Electronic Supplementary Information

The Marriage of endo-Cavity and exo-Wall Complexation Provides a Facile Strategy for Supramolecular Polymerization

Shilu Wang,[a] **Yiliang Wang,**[a] **Zhenxia Chen,**[*b] **Yuejian Lin,**[b] **Linhong Weng,**[b] **Kang Han,**[a] **Jian Li,**[a] **Xueshun Jia**[*a] **and Chunju Li**[*a,c]

[a] Department of Chemistry, Shanghai University, Shanghai, 200444, P. R. China; E-mail: cjli@shu.edu.cn; xsjia@mail.shu.edu.cn.

[b] Department of Chemistry, Fudan University, Shanghai 200433, P. R. China. E-mail: zhxchen@fudan.edu.cn.

[c] State Key Laboratory of Molecular Engineering of Polymers, Fudan University, Shanghai 200433, P. R. China.

Contents

Materials and methods.

per-Butylated pillar[5]arene (**1**) and N,N'-bis(*n*-butyl)pyromellitic diimide (**2**) were prepared by literature methods and recrystallized and dried under reduced pressure before use[S1]. Ditopic guest **3** was prepared according to our reported procedure.[S2] Solvents were either employed as purchased or dried according to procedures described in the literature. ^{1}H NMR, ^{13}C NMR, and DOSY spectra were recorded on a Bruker AV500 instrument. Viscosity measurements were carried out with Ubbelohde micro dilution viscometers (Shanghai Liangjing Glass Instrument Factory, 0.40 mm inner diameter) in chloroform. Electrospun supramolecular polymer nanofibers were obtained under the following conditions, 18 kV, 1.0 mL/h syringe flow rate, and 10 cm working distance, from a concentrated solution (~ 0.8 M) of 1_2•**2**•**3** in CHCl$_3$.

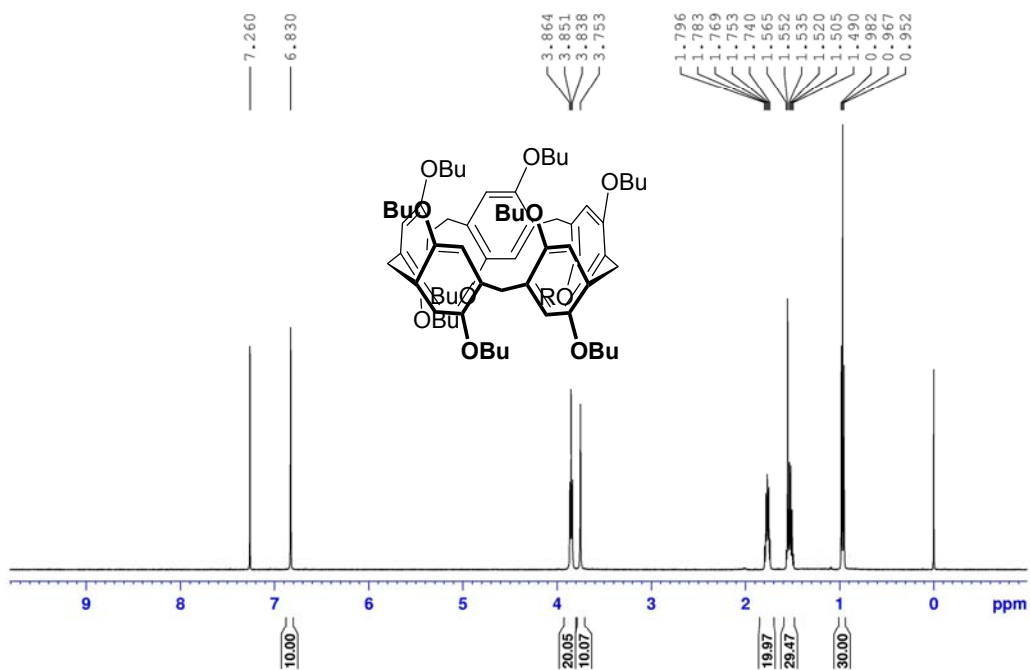# Copies of ^{1}H NMR and ^{13}C NMR spectra.

Figure S1. ^{1}H NMR spectrum (500 MHz) of **1** in CDCl$_3$.
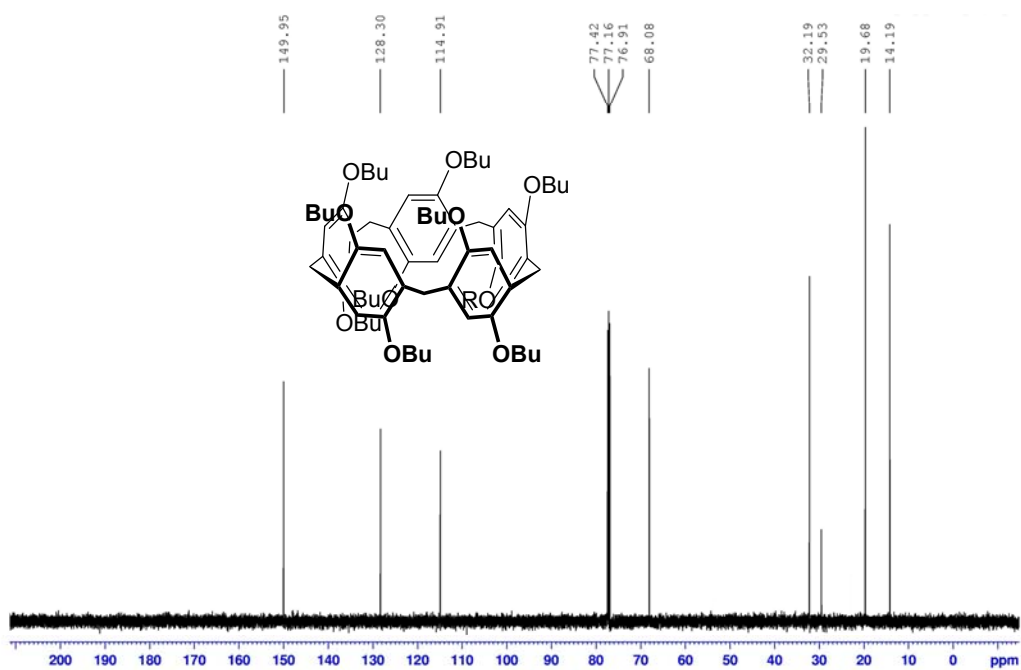
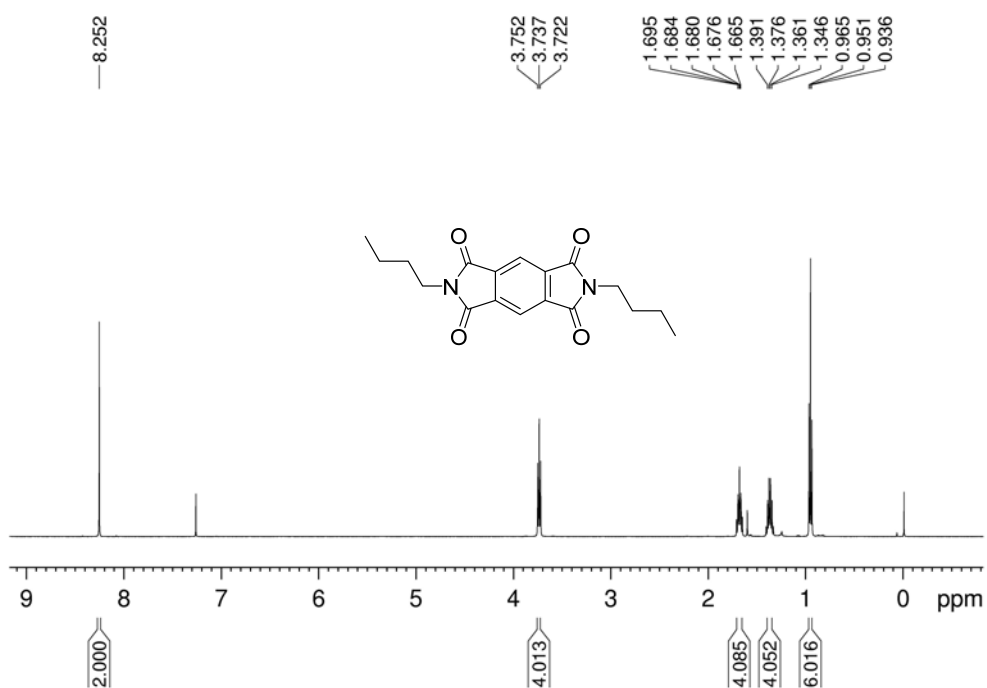**Figure S2.** ^{13}C NMR spectrum (125 MHz) of **1** in CDCl$_3$.

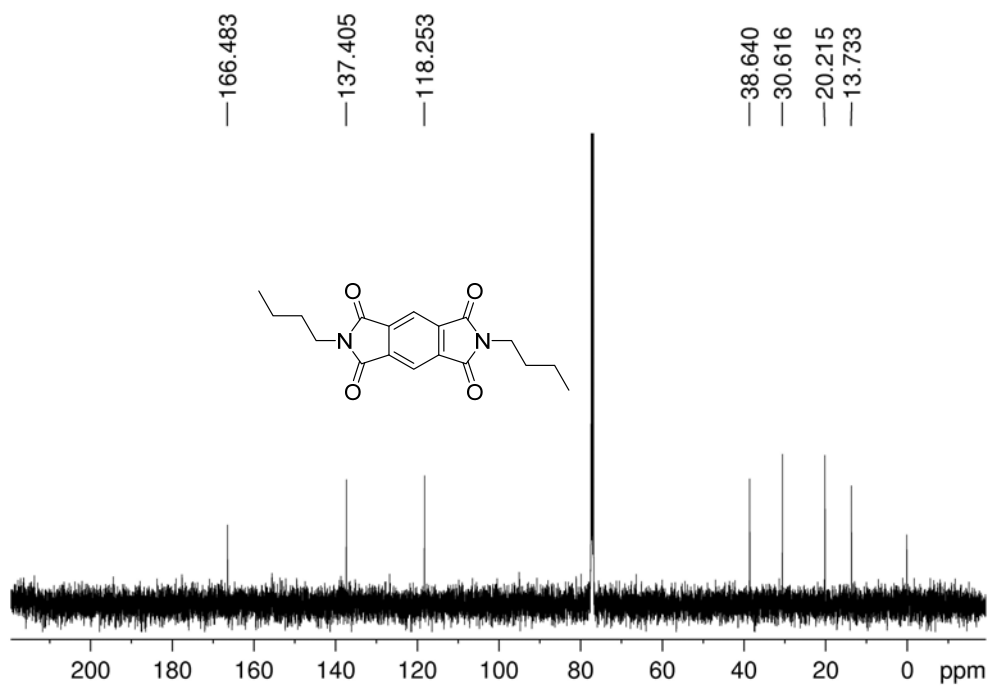**Figure S3.** ^{1}H NMR spectrum (500 MHz) of **2** in CDCl$_3$.

Figure S4. ^{13}C NMR spectrum (125 MHz) of **2** in CDCl$_3$.
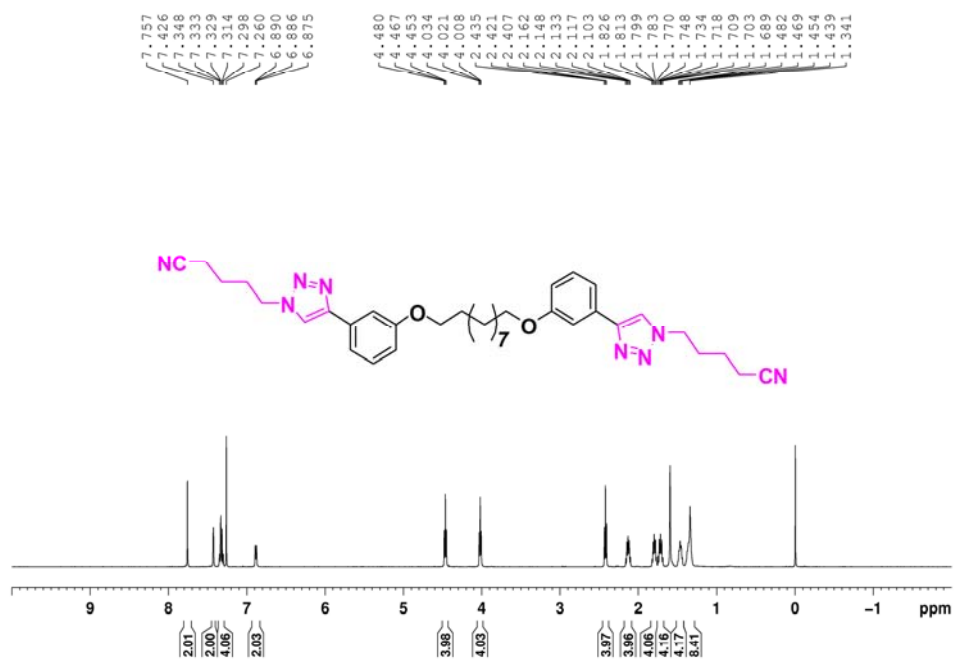
Figure S5. ^{1}H NMR spectrum (500 MHz) of **3** in CDCl$_3$.

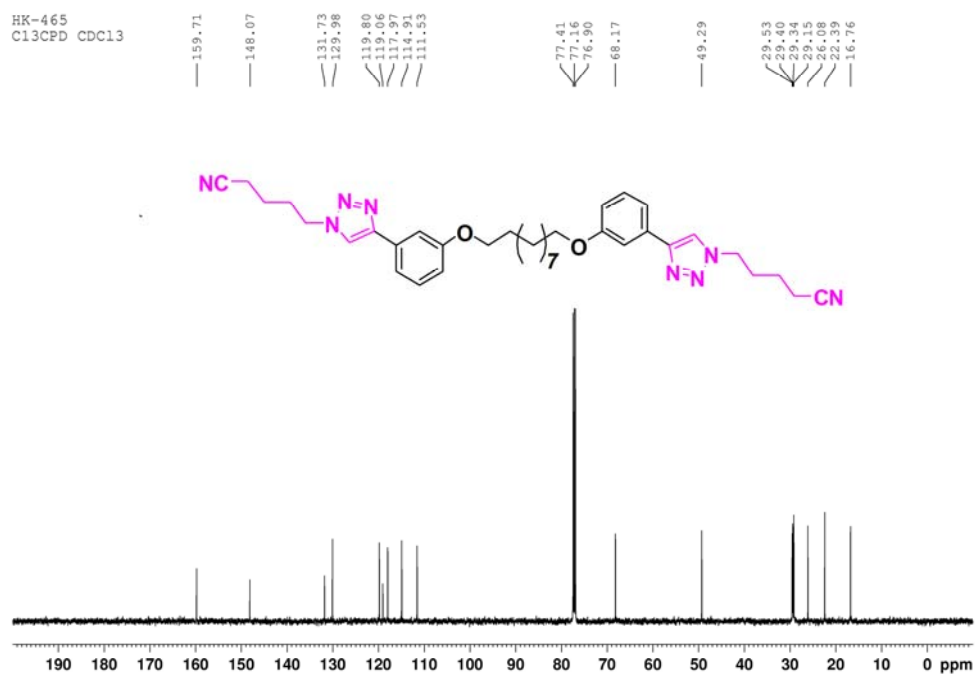**Figure S6.** ^{13}C NMR spectrum (125 MHz) of **3** in CDCl$_3$.
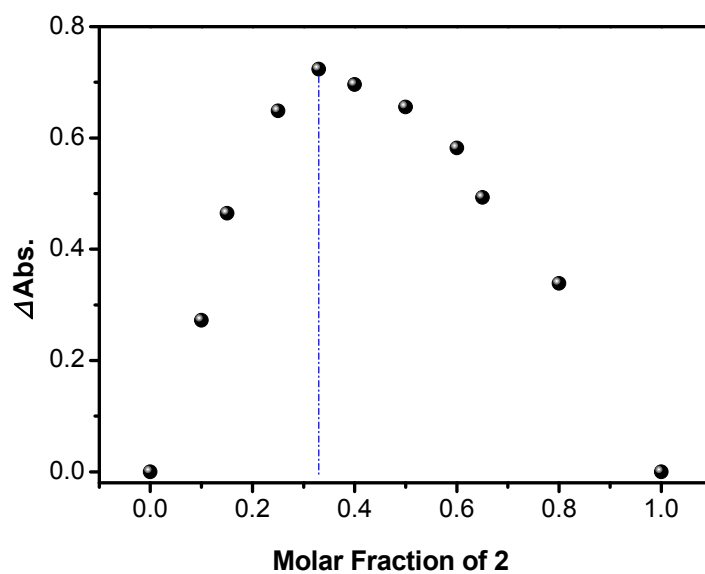
Job plot of 1/2 complexes.

Figure S7. Job plots showing the 2:1 stoichiometry of the complex between **1** and **2** in CHCl$_3$ by plotting the absorbance intensity at $\lambda = 482$ nm (the charge transfer band) against the mole fraction of **2** ([**1**] + [**2**] = 0.090 M)

X-ray crystal data and crystal structure of EtP5A$_2$•2 complex.

X-ray crystal data for EtP5A$_2$•2 complex.

Crystallographic data: red, C$_{64}$H$_{88}$NO$_{16}$, *FW* 1127.35, Triclinic, space group *P*-1, a = 12.306(7), b = 12.532(7), c = 25.592(14), α = 95.097(8)°, β = 99.985(8)°, γ = 107.517(8)°, *V* = 3665(4) Å^3, *Z* = 2, *D*$_c$ = 1.022 g cm^{-3}, *T* = 296(2)K, *μ* = 0.073 mm^{-1}, 19017 measured reflections, 12751 independent reflections, 730 parameters, 4 restraint, *F*(000) = 1214, *R*$_1$ = 0.2598, *wR*$_2$ = 0.5059 (all data), *R*$_1$ = 0.1742, *wR*$_2$ =0.4488 [*I* > 2σ(*I*)], max. residual density 1.401 e·Å^{-3}, and goodness-of-fit (*F*^{2}) = 1.521. CCDC 995204.
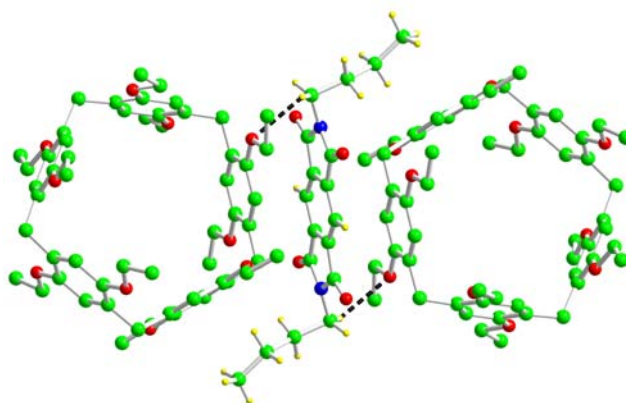

Figure S8. Crystal structure of EtP5A$_2$•2 complex. Oxygens are red, nitrogens are blue, carbons are green, and hydrogens are beige. Dashes represent C−H···O hydrogen bonds. H···O distance is 2.72 Å and C−H···O angle is 131 deg.
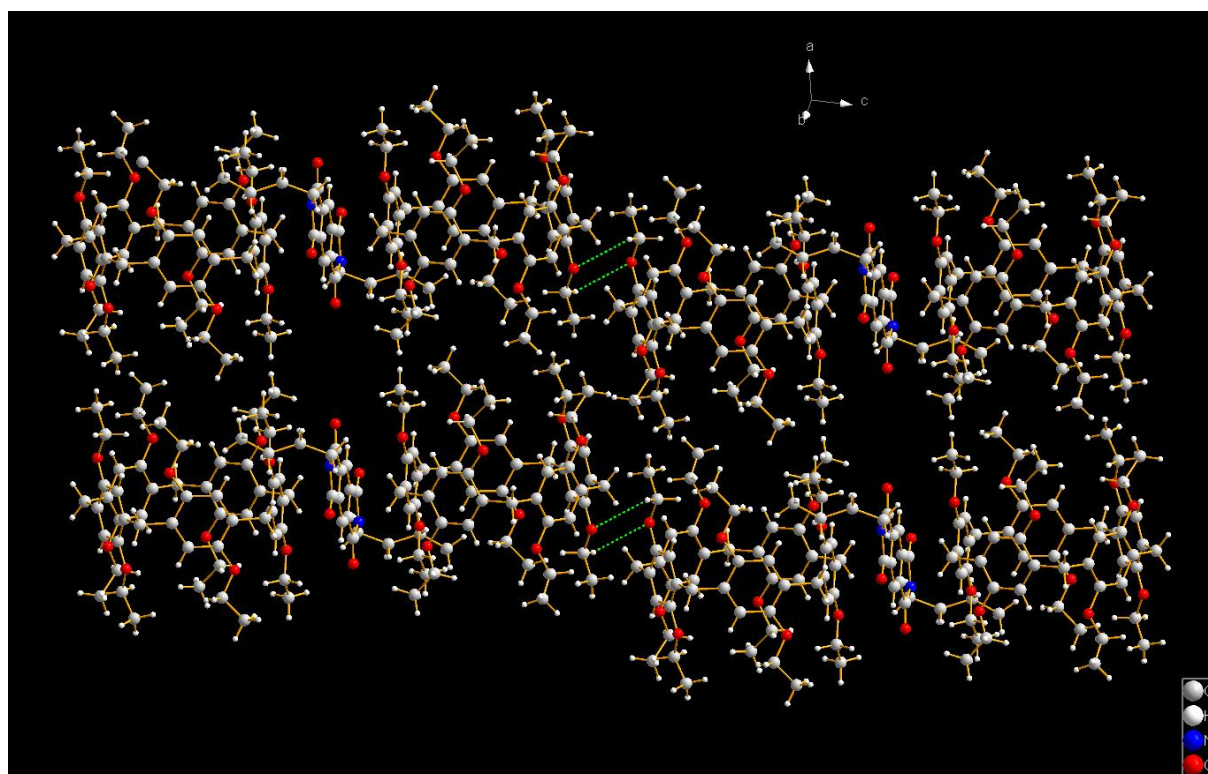
Figure S9. The packing structure of EtP5A$_2$•**2** complex. Dashes represent C−H···O hydrogen bonds between two neighboring EtP5A$_2$•**2** units. H···O distance is 2.99 Å and C−H···O angle is 129 deg.

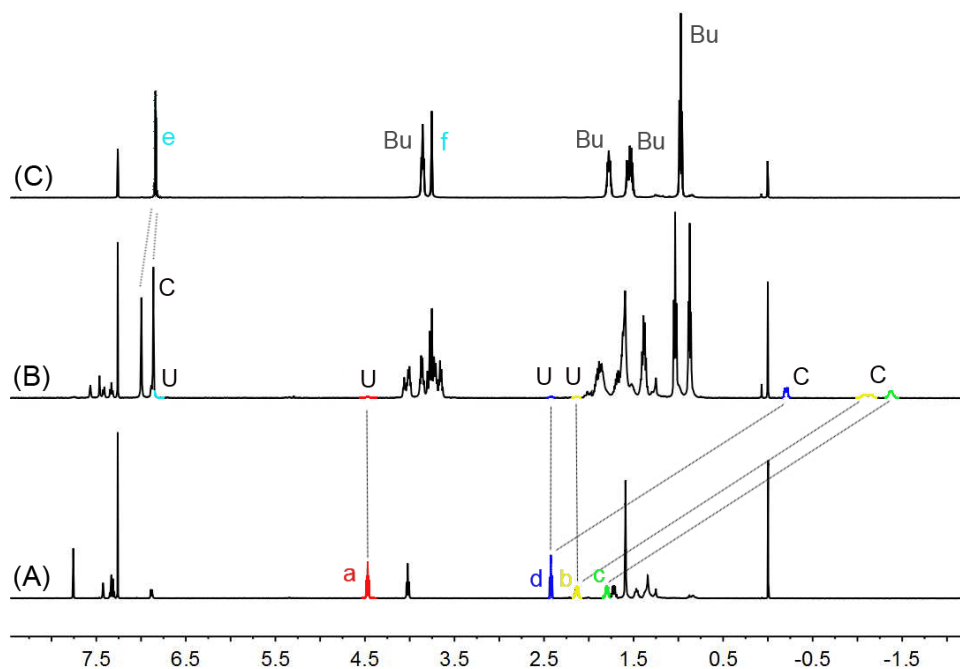**^{1}H NMR spectra of guest 3 in the absence and presence of P5A host 1.**

Figure S10. ^{1}H NMR spectra (500 MHz, CDCl$_3$, 298 K) of **3** (5.0 mM) upon complexation with 2.0 eq. of **1**. (A) **3** (B) **3** + **1**, and (C) **1**. "C" and "U" represent complexed and uncomplexed host/guest.

Figure S10 shows the ^{1}H NMR spectra of guest **3** in CDCl$_3$ in the absence and presence of 2.0 eq. of **1**. Slow exchange on the NMR timescale was observed for this complex. The resonances of the new species are consistent with the formation of a [3]pseudorotaxane-type interpenetrated complex. From integrations of all peaks, the stoichiometry of the complex between **1** and **3** can be determined to be 2 : 1. The peaks for the butylene protons of **3** (H$_{a-d}$) exhibit substantial upfield shifts and broadening effects compared to the free axle ($\Delta\delta$= −3.24, −3.17 and −2.63 ppm for H$_b$, H$_c$ and H$_d$, respectively) as a consequence of inclusion-induced shielding effects, indicating that the wheels is fully threaded by the butylene moieties. ^{1}H NMR results gave clear evidence for the formation of [3]pseudorotaxane **1$_2$•3**.

Determination of the association constant of 2 with [3]pseudorotaxane $1_2 \cdot 3$.

To quantitatively assess the exo-wall complexation behavior between **2** and [3]pseudorotaxane $1_2 \cdot 3$, UV-*vis* dilution experiments were performed at 298 K in chloroform solution. Using a well-defined (linear fitting) method, [S3] The association constant (K_a) could be obtained by analyzing the sequential changes in the absorbance (Abs.) of the complex at 460 nm that occurred with changes in concentration, [C], according to the following equation:[S3]

$$[C]/\text{Abs.} = (1/K_a \varepsilon l)^{1/2}(1/\text{Abs.})^{1/2} + 1/\varepsilon l$$

A plot of [C]/Abs., against $1/(\text{Abs})^{1/2}$ for a series of solutions of concentrations, is linear; the slope equals to $(1/K_a \varepsilon l)^{1/2}$ and the intercept equals to $1/\varepsilon l$. Typical UV spectrum changes and linear fitting plots are shown in Figure S11. It should be pointed out that, since the K_a value of 5-(1*H*-1,2,3-triazol-1-yl)pentanenitrile (TAPN) moiety with alkylated P5A is in the magnitude of 10^4 M^{-1},[S2] the uncomplexed P5A **1** in the formation of [3]pseudorotaxane $1_2 \cdot 3$ is less than 5% in the present operating concentrations ($10^{-3} - 10^{-2}$ M^{-1}) and is ignored in the determination of the K_a value between **2** and $1_2 \cdot 3$.
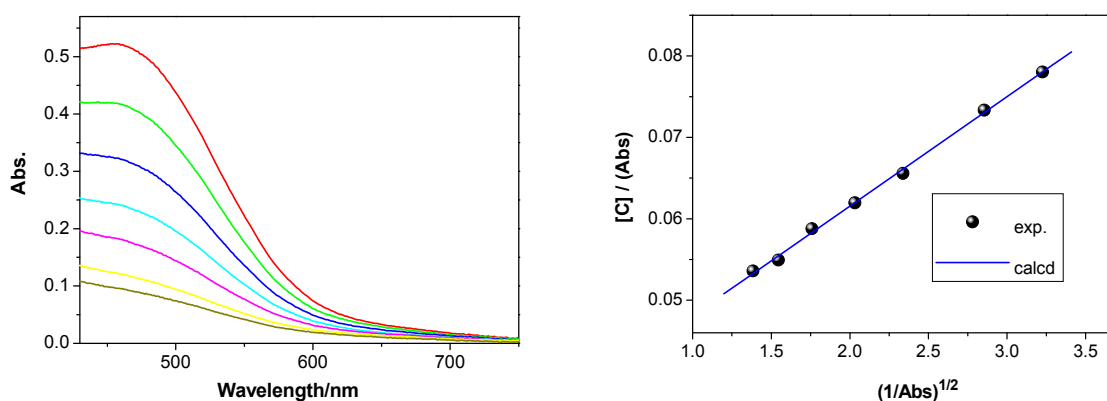

Figure S11. UV-*vis* spectra of **2** with [3]pseudorotaxane $1_2 \cdot 3$ at a series of concentrations (left), and the corresponding linear fitting plot (right).

Solution colors of the supramolecular polymer at different concentrations.
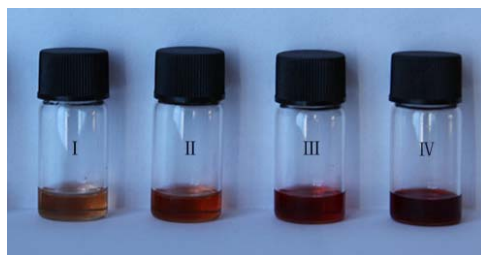

Figure S12. Concentration-dependent color changes of $1_2 \cdot 2 \cdot 3$ supramolecular aggregates in chloroform. (I) 35 mM; (II) 50 mM; (III) 100 mM; and (IV) 250 mM.
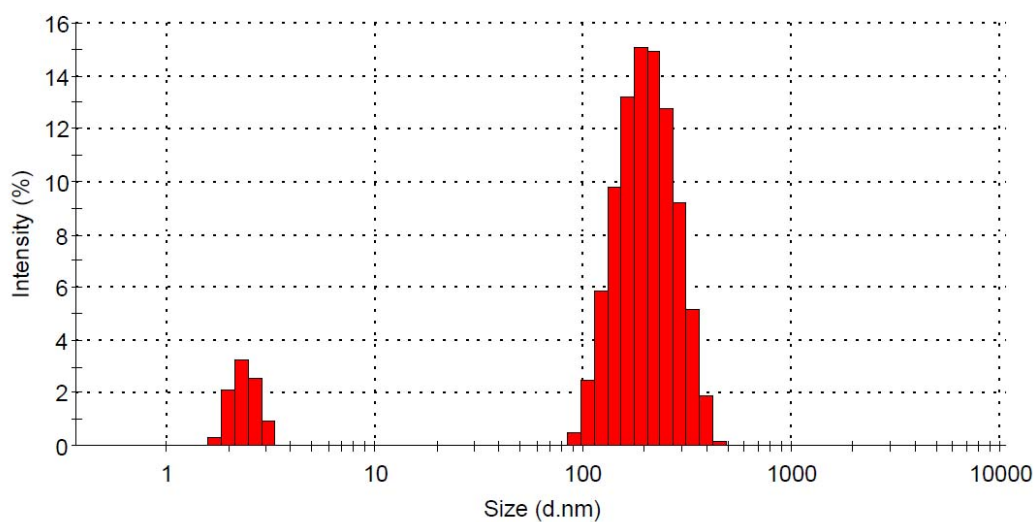
DLS experiments.

Figure S13. Hydrodynamic diameter distribution of supramolecular polymer $1_2 \cdot 2 \cdot 3$ (250 mM) in chloroform solution.

^{1}H NMR spectra of $1_2•2•3$ complex at various concentrations.

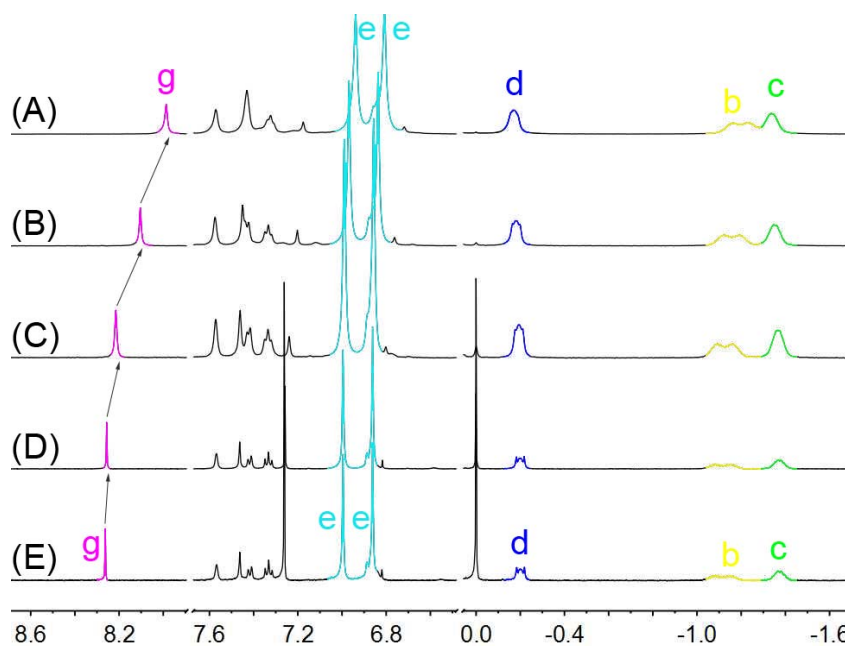**Figure S14.** Patial ^{1}H NMR spectra of $1_2•2•3$ complex (CDCl$_3$, 500 MHz, 298 K) at various concentrations: (A) 250 mM; (B) 100 mM; (C) 35 mM; (D) 10 mM; (E) 2.5 mM.

References.

[S1] (a) Swati De, S. Ramakrishnan, *Macromolecules* **2009**, *42*, 8599–8603. (b) T. Ogoshi, S. Kanai, S. Fujinami, T. Yamagishi, Y. Nakamoto, *J. Am. Chem. Soc.* **2008**, *130*, 5022–5023.

[S2] C. Li, K. Han, J. Li, Y. Zhang, W. Chen, Y. Yu, and X. Jia *Chem.–Eur. J.*, **2013**, *19*, 11892–11897.

[S3] (a) K. A. Connors, Binding Constants; Wiley: New York, **1987**. Corbin, P. S. Ph.D. Dissertation, University of Illinois at Urbana-Champaign, Urbana, IL, 1999; (b) Swati De, S. Ramakrishnan, *Chem.–Asian J.* **2011**, *6*, 149–156.